Automated cement segmentation in vertebroplasty

Nina Kozic MSc [a,*], Stefan Weber PhD [a], Miguel Á. González Ballester PhD [b], German Abdo MD [c], Daniel A. Rüfenacht MD [d], Stephen J. Ferguson PhD [a], Mauricio Reyes PhD [a]

[a] *Institute for Surgical Technology and Biomechanics, Bern, Switzerland*

[b] *Alma IT Systems, Barcelona, Spain*

[c] *Hospital de los Valles, Quito, Ecuador*

[d] *Hirslanden Clinic, Neuroradiology Department, Zürich, Switzerland*

Abstract

Vertebroplasty is a minimally invasive procedure with many benefits. However, the procedure is not without risks and complications. Leakage of the cement out of the vertebral body and into the surrounding tissues is one of the most serious complications of vertebroplasty. Cement can leak into spinal canal, venous system, soft tissues, lungs and intradiscal space, causing serious neurological complications, tissue necrosis or pulmonary embolism. In this work we present a method for automatic segmentation and tracking of bone cement during vertebroplasty procedures, as a first step towards building a warning system to avoid cement leakage outside the vertebral body. We show that using active contours based on level sets the shape of the injected cement can be accurately detected. We have improved the model for segmentation proposed in our previous work, by including a term that restricts the level set function to the vertebral body. We have applied the method to a set of real intra-operative X-ray images and our results show that the algorithm can successfully detect different shapes with blurred and not well defined boundaries, where the classical active contours segmentation is not applicable. The method was positively evaluated by physicians.

Key words: Vertebroplasty, cement segmentation, level sets

* Corresponding author. Address: Institute for Surgical Technology and Biomechanics, University of Bern, Stauffacherstrasse 78, 3014 Bern, Switzerland. Tel: 41 31 631 59 50. Fax: 41 31 631 59 60. E-mail: kozic.nina@gmail.com; mauricio.reyes@istb.unibe.ch.

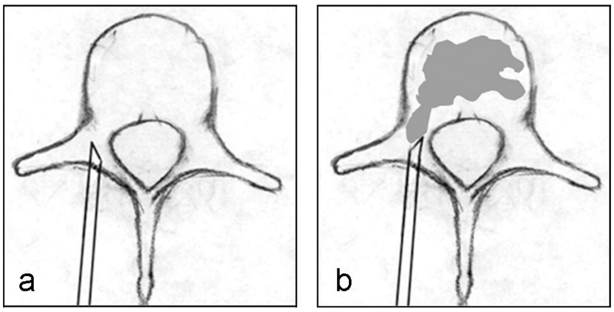

Fig. 1. Schematic drawings of vertebroplasty procedure: (a) Vertebroplasty needle is inserted through the pedicle of the vertebra. (b) Acrylic bone cement is injected into the vertebra, filling the cavity within the bone [4].

Introduction

Vertebroplasty is a minimally invasive image-guided procedure in which a biomaterial (bone cement) is injected into the spine in order to stabilize fractured vertebra and relieve pain (Figure 1) [1–4]. Problems that could be treated by this procedure include painful compression fractures resulting from osteoporosis, fractures associated with cancer or benign blood vessel expansions, and fractures from trauma. During image guided vertebroplasty procedures, cement injection is monitored using X-ray imaging. However, the visibility on the screens of the operating room could be poor and it may be very difficult and time consuming for the surgeon to detect the borders of the injected cement. Furthermore, especially when using old imaging equipment, only very experienced physicians are able to accurately visualize the cement and distinguish it from bony structures.

Leakage of the cement out of the vertebral body and into the surrounding tissues is one of the most serious complications in vertebroplasty (Figure 2) [5–7]. In a large number of vertebroplasty cases, cement leakage is detected only after the procedure. Most common problems include pulmonary embolism [8] and fractures of adjacent vertebral bodies [9]. Leakage into the spinal canal and nearby nerves may cause serious neurological complications potentially leading to death if the cement enters the blood stream [10].

In certain cases, an intraosseous venography can be used, prior to cement injection, to map the venous outlets from the vertebral body [1,3]. In this way the surgeon can reposition the vertebroplasty needle, if injection of the contrast agent shows a large direct venous connection. Although venography can show sites of potential leakage, stagnant contrast agent makes the cement

---

Part of this research was previously presented at the 20th International Conference on Computer Assisted Radiology and Surgery (CARS 2006), held in Osaka, Japan, on 28 June - 1 July 2006.

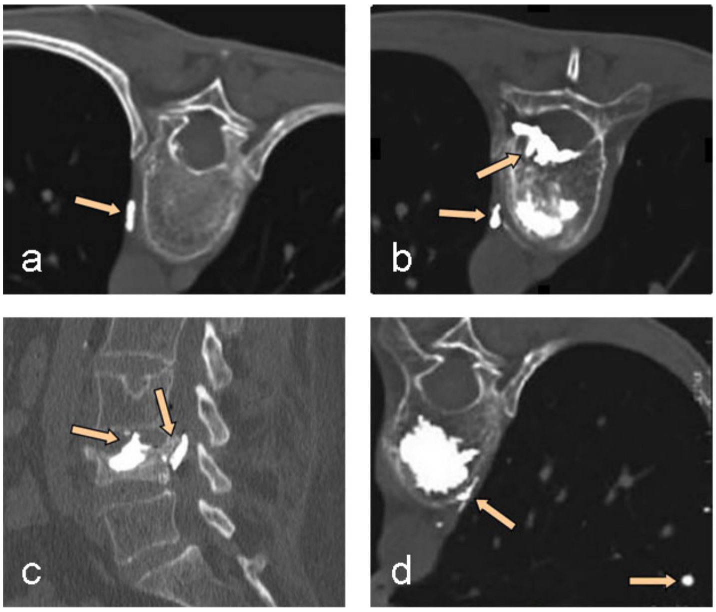

Fig. 2. Leakage of cement during vertebroplasty procedures: (a) Leakage through the vertebral venous system. (b) Leakage through epidural space. (c) Leakage into intervertebral discs. (d) Leakage in surrounding tissues (pulmonary). (images courtesy of The Inteventional Radiology website and National Naval Medical Center - WebMedpix)

injection more difficult to monitor, and an allergic reaction to contrast agent remains a potential risk. Furthermore, it has been shown that venography does not significantly increase the effectiveness or safety of percutaneous vertebroplasty [11,12] and opinions about the utility of venography to improve clinical outcomes or decrease complications during vertebroplasty are controversial.

Hence, it is of paramount importance to monitor the evolution of the injected cement. In this work, we propose a method for automated cement segmentation and tracking on fluoroscopic X-ray images, to help predict eventual leakage and stop the injection if necessary. The method was tested on a set of X-ray images obtained during real vertebroplasty procedures performed in the Radiology Department of University Hospital of Geneva, and was positively evaluated by physicians.

Methods

Segmentation techniques based on active contours [13], or deformable models, have been widely used in image processing for different medical applications, such as computer integrated surgery or computer aided diagnosis [14]. The idea behind active contours is to extract the boundaries of homogeneous regions within the image, while keeping the model smooth during deformation. In such models, the initial contour, specified by the user, is evolved to the boundaries of the object by balancing two energy forces. The first force, computed from image data, represents external energy that attracts the curve towards image features, while the second force, defined within the curve, represents the internal energy and affects the smoothness of the curve. Using classical active contours with an edge-stopping function [15] can greatly affect the segmentation of the model with diffuse and not well defined edges, especially if the deformation involves splitting or merging of parts. In those cases, when the image topologies are unidentified, segmentation should be performed using an energy minimisation approach, which will be explained in the following subsections.

Mumford-Shah model

One of the most extensively studied mathematical models for medical image segmentation is the variational model of Mumford and Shah [16–18], which detects an object via minimization of an energy functional involving a piecewise smooth approximation of the image. The problem can be additionally reduced by restriction of the segmented image to piecewise constant image functions on each segmented region. This simplified case is called the minimal partition problem, and in order to solve it Mumford and Shah propose to minimize the following functional:

$$F^{MS} = \sum_i \lambda_i \int_\Omega |u_0(x,y) - c_i|^2 dxdy + \mu|C| \tag{1}$$

where C is a finite set of closed, smooth curves in a bounded region $\Omega \in \mathcal{R}^2$, with total length $|C|$, $u_0 : \Omega \to \mathcal{R}$ represents the observed image and c_i is the approximation to piecewise constant image functions, $c_i = mean(u_0)$, on each segmented region $\Omega_i \subset \Omega$. λ_i and μ are positive parameters that regulate the balance between energies.

Cement segmentation based on level sets

The energy functional proposed by Mumford and Shah is not easy to solve because of the unknown set of complex contours C and unidentified image topologies. The segmentation algorithm developed in this work is based on the implicit representation of deformable models implemented within the framework of level sets, as it is proposed by Chan and Vese [17]. This implicit representation for evolving curves, introduced by Osher and Sethian [19], allows automatic change of topologies without re-parametrization.

Let $\omega \subset \Omega$ be the region inside the curve. Using the level set formulation, the boundary $C = \partial\omega$ can be modelled as a zero level set of a Lipschitz function ϕ, defined on the entire image domain Ω as: $C = \partial\omega = \{x \in \Omega : \phi(x) = 0\}$, $inside(C) = \omega = \{x \in \Omega : \phi(x) > 0\}$ and $outside(C) = \Omega \setminus \omega = \{x \in \Omega : \phi(x) < 0\}$. Having the Heaviside function $H(\phi)$ defined on the whole image domain Ω, and its corresponding Dirac function $\delta(\phi)$, we can replace the unknown variable C by the level set function $\phi(x)$ as:

$$\begin{aligned} F(\phi, c_1, c_2) = \mu \int_\Omega \delta(\phi)|\nabla\phi| + \lambda_1 \int_\Omega |u_0 - c_1|^2 H(\phi) d\Omega \\ + \lambda_2 \int_\Omega |u_0 - c_2|^2 (1 - H(\phi)) d\Omega, \end{aligned} \tag{2}$$

where the length value $|C| = \int_\Omega \delta(\phi)|\nabla\phi|$ is estimated directly from the level set function [20]. In Figure 3 we show how our segmentation algorithm works on X-ray scans during cement injection in vertebroplasty (see [21] for more detailed discussion on model implementation).

Model restriction to vertebral shape

In this work we propose a modification of the functional defined above by restriction of the level set function to the area of interest, which in our case is the vertebral body. Introducing a mask term in the functional, the performance of the model is improved. Segmentation of objects outside of the vertebral body is thus effectively avoided, by detecting when segmented cement approaches the borders of the vertebra (Figure 3).

Let m be a mask defined as $m(x, y) = 0$ inside the vertebral body and $m(x, y) = 1$ outside. Our energy functional can be modified as follows:

$$\begin{aligned} F(\phi, c_1, c_2) = \mu \int_\Omega \delta(\phi)|\nabla\phi| + \lambda_1 \int_\Omega |u_0 - c_1|^2 H(\phi) d\Omega \\ + \lambda_2 \int_\Omega |u_0 - c_2|^2 (1 - H(\phi)) d\Omega + \lambda_3 \int_\Omega m H(\phi) d\Omega \end{aligned} \tag{3}$$

Finally, the boundary is updated by solving a nonlinear, model associated Euler-Lagrange equation:

$$\begin{aligned} \frac{\partial\phi}{\partial t} = \mu\delta_0(\phi) div \left(\frac{\nabla\phi}{|\nabla\phi|} \right) \\ + \delta_0(\phi) \sum_{i=1}^{2} (-1)^2 \lambda_i (u_0 - c_i)^2 + \lambda_3 \delta_0(\phi) m = 0 \end{aligned} \tag{4}$$

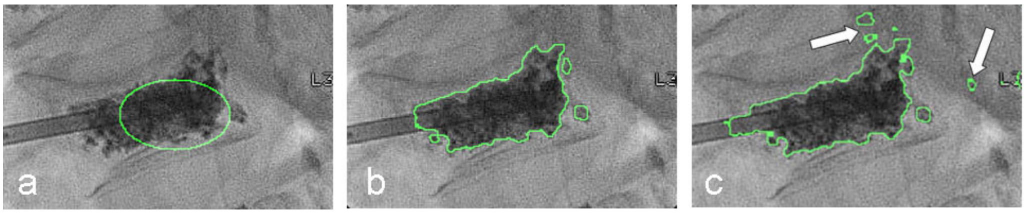

Fig. 3. (a) Original image with the initialization contour. b) Result after 400 iterations. c) Result after 700 iterations, showing that the segmentation incorrectly extends out of the vertebral body.

At each iteration step, a level set deformation is computed as a variation of mean curvature of the level set ϕ, the first term in Eq. (4), and as a piecewise smooth approximation of the image data inside and outside the contour, the second term in Eq. (4). The mask term penalizes the evolution of the contour outside of the region of interest and assures convergence of energy.

Results

We have applied our method to a set of X-ray images obtained during real vertebroplasty procedures performed in the Department of Radiology and Medical Computing at the University Hospital of Geneva. The images were obtained using a Philips V5000 B-plane Integres C-arm and show sagittal scans of the vertebral body during cement injection. We have tested our method in a total of 13 scans, corresponding to 4 vertebrae (L2, L3 and L4), at different time steps during injection (between the 3rd and 8th minute), and depicting a variety of cement shapes. The images were filtered by anisotropic diffusion prior to segmentation, in order to reduce the noise of the low quality X-ray images and encourage smoothing in homogeneous regions while preserving edges [22].

Initialization was performed by automatically selecting the center, as the midpoint of the image, and the radius of the initial curve, which in our case was an ellipse with the axes as 1/3rd of the image size (Figure 3a). The energy parameter values are chosen empirically as follows: $\mu = 325$, $\lambda_1 = 0.3$, $\lambda_2 = 0.7$, and $\lambda_3 = 1000$. The algorithm was implemented in Matlab and the images shown here are obtained after 150 iterations, which approximately takes 7 seconds (CPU @1.7GHz, RAM 512MB).

We present the results on a third lumbar vertebra with osteoporosis in four different time points during injection of bone cement (Figure 4). In Figure 4a, we show the original images, in which we can observe the cannula inserted in the vertebral body and the injected cement. In Figure 4b we show the resulting segmentation contour in light green. The bottom row corresponds

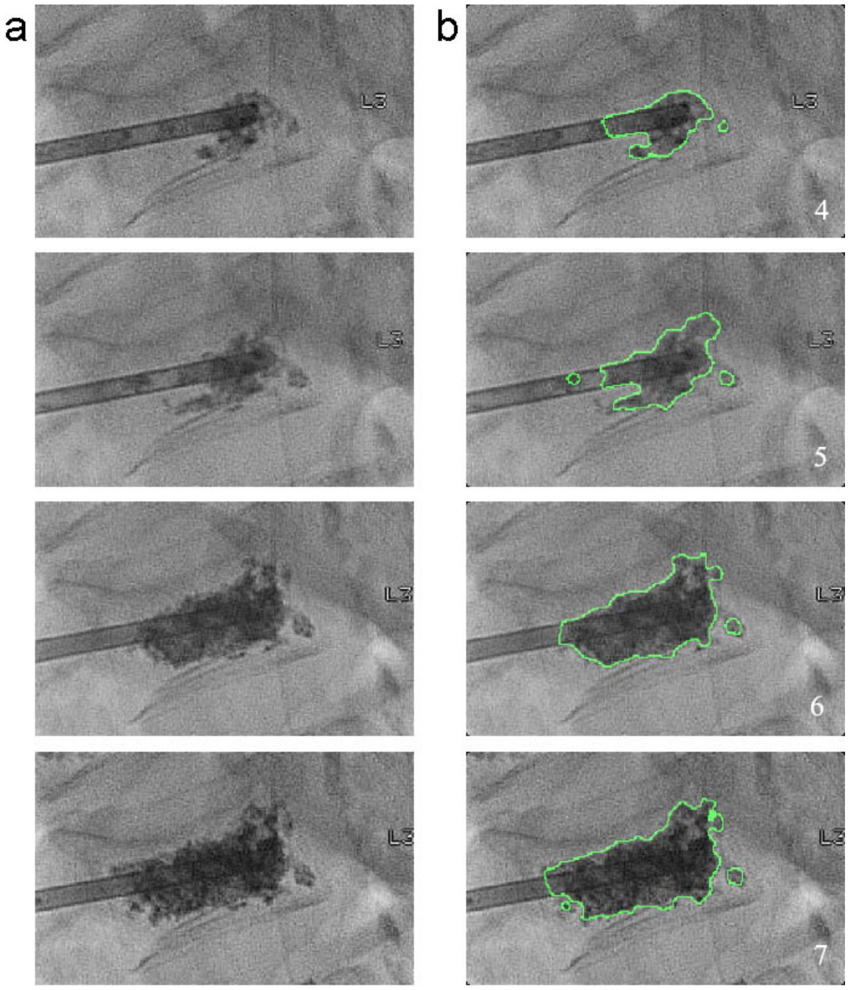

Fig. 4. (a) Image sequence during cement injection in lumbar vertebra L3. (b) Segmentation results.

to the same image as in Figure 3b, and it shows that our algorithm performs much better than the one without mask restriction (compare to Figure 3c). The convergence of the energy was observed after 500 iterations (25 seconds), as opposed to the case of the algorithm without mask restriction, which fails to converge. In all the tested images, no noticeable differences in contour shape were visible when comparing the result after 500 iterations with that after 150 iterations, which only takes 7 seconds.

Our results have been evaluated by the interventional radiologist that performed the operations. The scale, based on clinical usability, was as follows: 1-very bad, 2-bad, 3-satisfying, 4-good and 5-very good. The physician would evaluate the result as bad even if the overall segmentation was correct, but even a small particle of the cement was not detected, since this can potentially lead to leakage and serious complications. Based on this evaluation scale, the segmented sequence in Figure 4, obtained during cement injection in third lumbar osteoporotic vertebra, was evaluated as 5, 4, 5 and 5 top-down. We

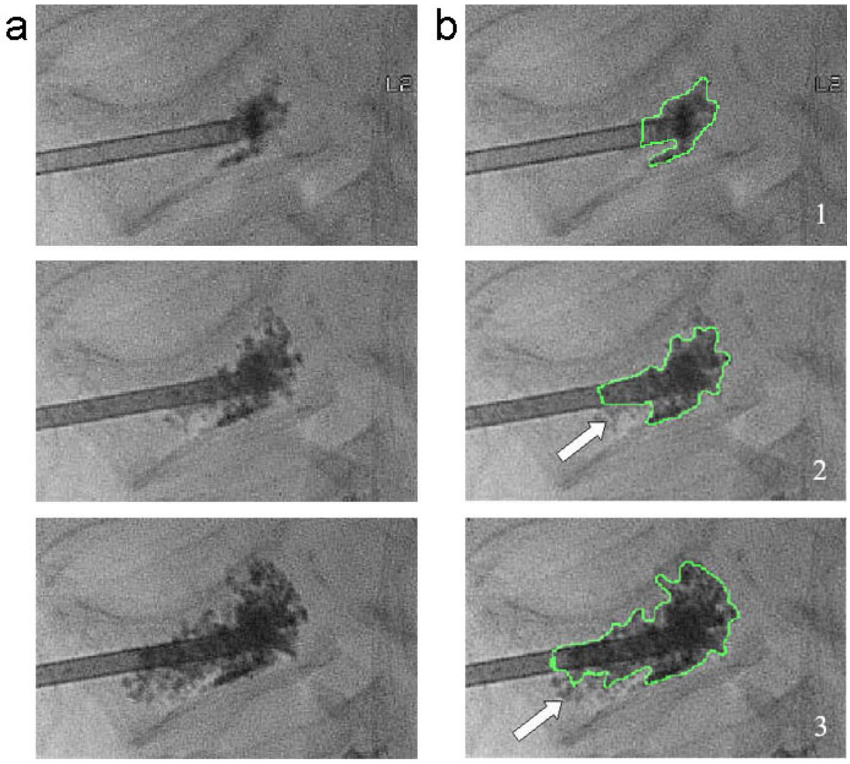

Fig. 5. (a) Image sequence during cement injection in lumbar vertebra L2. (b) Segmentation results.

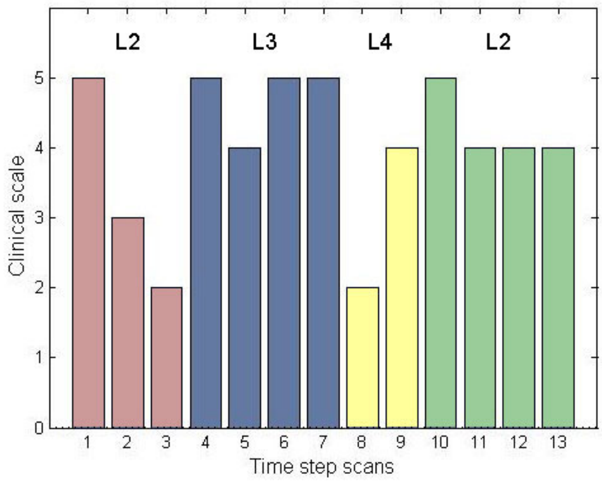

Fig. 6. Evaluation of cement segmentation on 13 X-ray images (time step scans), corresponding to 4 vertebrae (shown in different colors). The scale, based on clinical usability, was: 1-very bad, 2-bad, 3-satisfying, 4-good and 5-very good.

show another example of algorithm performance on an osteoporotic second lumbar vertebra (Figure 5). This sequence was evaluated as 5, 3 and 2, since a certain amount of cement (indicated by arrows) was not detected. Clinical evaluation of all 13 cement segmentations is shown in Figure 6.

Discussion

Leakage of the cement outside of vertebral body may lead to serious postoperative problems for the treated person and it is of paramount importance to correctly monitor the evolution of injected cement. We have developed a method for automatic cement segmentation during vertebroplasty procedures. The algorithm performs very well, in terms of speed and accuracy, on objects with blurred and not well defined boundaries, as is the case of the cement, where the classical active contours segmentation is not applicable. Validation of the results by the surgeon proves the utility of this technique.

One of the strengths of this method is that it can detect several contours in one image, thus tracking cement particles that spread out of the main cement cloud. This is very important for detecting the leakage of cement during the surgery and it can be a signal to the physician to stop the injection. We show as well one of the drawbacks of our algorithm (Figure 5b). In these cases the distribution of cement is more spread out than in other cases and there is a higher gradient close to the cannula edges which affects internal energy and curve evolution. One of the possible solutions for resolving this problem would be to segment the cannula, subtract it from the images and smooth the intensities around cannula.

The incorporation of the mask term significantly improves the performance of the algorithm, but it naturally leads to the need for an automatic segmentation of vertebrae. This is a focus of our future research. The method has now been applied to a set of static images extracted from real injection sequences, but further evaluation on real-time dynamic sequences using GPU-enabled technologies is currently in progress.

We believe that the development of an automatic warning system for cement leakage will improve the safety of vertebroplasty and minimize potential complications.

Acknowledgements

This research was funded by the Swiss National Science Foundation through its National Center of Competence in Research (NCCR) on Computer Aided and Image Guided Medical Interventions (http://co-me.ch).

References

[1] Kallmes DF, Jensen ME. Percutaneous Vertebroplasty. Radiology 2003;229(1):27–36

[2] Burton AW, Rhines LD and Mendel E. Vertebroplasty and kyphoplasty: A comprehensive review. Neurosurgical Focus 2005;18(3):1–9

[3] Mehbod A, Aunoble S, Le Huec JC. Vertebroplasty for osteoporotic spine fracture: Prevention and treatment. Eur Spine J 2003;12:S155-S162

[4] Martin JB, Wetzel SG, Seium Y, Dietrich PY, Somon T, Gailloud P, Payer M, Kelekis A, Ruefenacht DA. Percutaneous Vertebroplasty in Metastatic Disease: Transpedicular Access and Treatment of Lysed PediclesInitial Experience. Radiology 2003;229(2):593-597

[5] Schmidt R, Cakir B, Mattes T, Wegener M, Puhl W, Richter M. Cement leakage during vertebroplasty: An underestimated problem? Eur Spine J 2005;14(5):466–473

[6] Yeom JS, Kim WJ, Choy WS, Lee CK, Chang BS, Kang JW. Leakage of cement in percutaneous transpedicular vertebroplasty for painful osteoporotic compression fractures. J Bone Joint Surg 2003;85-B(1):83–89

[7] Hulme PA, Krebs J, Ferguson SJ, Berlemann U. Vertebroplasty and kyphoplasty: A systematic review of 69 clinical studies. Spine 2006;31(17):1983-2001

[8] Jang JS, Lee SH, Jung SK. Pulmonary embolism of poymethylmethacrylate after percuteneous vertebroplasty: A report of three cases. Spine 2002;27(19):E416–E418

[9] Lina EP, Ekholma S, Hiwatashia A, Westesson PL. Vertebroplasty: Cement Leakage into the Disc Increases the Risk of New Fracture of Adjacent Vertebral Body. AJNR Am J Neuroradiol 2004;25:175-180

[10] MacTaggart JN, Pipinos IIP, Johanning JM, Lynch TG. Acrylic cement pulmonary embolus masquerading as an embolized central venous catheter fragment. J Vasc Surg 2006;43(1):180–183

[11] Vasconcelos C, Gailloud P, Beauchamp NJ, Heck DV, Murphy KJ. Is percutaneous vertebroplasty without pretreatment venography safe? Evaluation of 205 consecutives procedures. AJNR Am J Neuroradiol 2002;23(6):913–917

[12] Do HM. Intraosseous venography during percutaneous vertebroplasty: is it needed? AJNR Am J Neuroradiol 2002;23(4):601–604

[13] Kass M, Witkin A, Terzopoulos D. Snakes: Active contour models. Int J Comput Vis 1980;1:321–331

[14] Wong A, Mishra A, Fieguth P, Clausi D, Dunk NM, Callaghan JP. Shape-Guided Active Contour Based Segmentation and Tracking of Lumbar Vertebrae in Video Fluoroscopy Using Complex Wavelets. Proc. IEEE Eng Med Biol Soc. 2008;2008:863-866

[15] Malladi R, Sethian JA, Vemuri BC. Shape modeling with front propagation: A level set approach. IEEE Trans Pattern Anal Mach Intell 1995;17(2):158–175

[16] Mumford D, Shah J: Optimal approximation by piecewise smooth functions and associated variational problems. Commun Pure and Applied Mathematics 1989;42:577–685

[17] Chan TF, Vese LA. Active Contours Without Edges. IEEE Trans Image Process 2001;10(2):266–277

[18] Tsai A, Yezzi A, Willsky AS. Curve Evolution Implementation of the Mumford-Shah Functional for Image Segmentation, Denoising, Interpolation, and Magnification. IEEE Trans Image Process 2001;10(8):1169–1186

[19] Osher S, Sethian JA. Fronts propagating with curvature-dependent speed: Algorithms based on Hamilton-Jacobi Formulation. J Comput Phys 1988;79:12–49

[20] Evans LC, Gariepy RF. Measure Theory and Fine Properties of Functions. Boca Raton, FL: CRC 1992.

[21] Kozic N, Abdo G, Rüfenacht DA, Nolte LP, Gonzalez Ballester MA. Automated Cement Segmentation in Vertebroplasty Based on Active Contours Without Edges. International Journal of Computer Assisted Radiology and Surgery 2006;1(S1):192–194

[22] Perona P, Malik J. Scale-Space and Edge Detection Using Anisotropic Diffusion. IEEE Trans Pattern Anal Mach Intell 1990;12(7):629–639

List of Figures